J. Inst. Eng. India Ser. B (October 2019) 100(5):435–445
https://doi.org/10.1007/s40031-019-00396-x

ORIGINAL CONTRIBUTION

GA-GNN (Genetic Algorithm-Generalized Neural Network)-Based Fault Classification System for Three-Phase Transmission System

Sanjeev Kumar Sharma[1]

Received: 1 June 2018 / Accepted: 8 March 2019 / Published online: 20 May 2019

Abstract This research paper proposes a synergetic approach for fault classification of a three-phase transmission system. The voltage signals of all three phases at generating bus of the transmission system are acquired and processed for different operating (healthy and unhealthy) conditions. The analysis of signals is done by Clarke transform and Fourier transform. Clarke transform is used for the detection of involvement of the ground in the fault. Various types of faults such as symmetrical faults and asymmetrical faults have been considered (faults among two phases, phase A and phase B (AB), phase B and phase C (BC) and phase C and phase A (CA), faults in different phases and ground, phase A and ground (AG), phase B and ground (BG), phase A, phase B and ground (ABG), etc.). The phase angle of the measured three-phase voltage at one point of the transmission line is calculated with Fourier transform and compared in order to distinguish the type of fault. These obtained features are then utilized by trained GA-GNN for differentiating various types of faults. The different types of fault data are summarized in a normalized matrix form, and this normalized matrix is fed as input to the fuzzy logic and GA-GNN. The method is very easy in implementation and obtained results show that the method is very accurate and has practicability.

Keywords Clarke transform · Fast Fourier transform · Genetic algorithm · Generalized neural network · Fault identification

✉ Sanjeev Kumar Sharma
sanjeev.eck@gmail.com

[1] JSS Academy of Technical Education, Noida, India

Introduction

The generating stations are located near the coal fields, which are generally far away from the electrical load centers, *i.e.,* end user of the electricity. The electrical power in bulk is produced in these generating stations. This power is transmitted from these generating stations to the load centers by means of three-phase transmission lines. The length of the power system transmission lines may vary from few kilometers to thousands of kilometers, and they are directly exposed to the external environment. Hence, the overhead transmission lines are very prone to the faults, *i.e.,* ten different types of fault can occur anywhere, any time on the transmission lines. As the transmission lines carry huge amount of power, even a slight disturbance may lead to the blackout of a substantial geographical area. These disturbances may lead to deterioration of quality of power supplied to the consumers. Therefore, a reliable and accurate method for fault detection, classification and isolation of the faulty section is required so that the supply can be restored as early as possible. Several techniques have been proposed by the researchers about the said problem, in last two decades.

The various methods have been published in the research literature by researchers, which are based upon Fourier transform, wavelet transforms, S-transform, Z-transform, etc. The Fourier transform-based methods of fault classification utilize the Fourier transform for analysis of the signals. Abdel Aziz et al. [1] proposed a Fourier transform-based method, which employs the third-harmonic components only, and based upon third-harmonic components, three different models have been developed. Samantaray [2] presented an S-transform and fuzzy logic-based fault classification method. The concept of S-transform uses the concept of wavelet transform. The phase

space information of the phase current signal is adopted. The method suffers inherent disadvantages of the transform and fuzzy logic. Dasgupta et al. [3] presented a method which is based upon wavelet entropy and artificial neural network (ANN). But, the ANN takes a longer duration in conversing, if the data set is huge. Majid Jamil et al. [4] presented a wavelet spectral energy and GNN-based method of fault location. Pradhan et al. [5] proposed a discrete wavelet transform-fuzzy logic-based approach for series capacitor-compensated transmission line, but this method is complex and not accurate for boundary line cases, where the difference in between two faults data is very near to each other. The various hybrid techniques based upon fuzzy logic, soft computing, neural network, adaptive network, etc, are discussed in [6–10]. Moravejb et al. proposed an idea for fault detection and fault classification of a power system transmission line, which is based upon the combination of hyperbolic S-transform and learning machine (*i.e.,* ANN) using one cycle current and voltage signals of three phases. The method is complicated as the numbers of input samples is doubled because both the current and the voltage are required for fault classification [10]. Jayabharata Reddy et al. [11] presented a model of fault detection and location, which is based upon wavelet transform and fuzzy logic. Rizwan et al. [12] discussed the method of feed forward neural network, which is combined with wavelet transform in fault location calculations. Alanzi et al. [13] proposed a method, which is based upon comparison of phase shift angle of measured voltage signal, but the algorithm is not as effective as, when the numbers of fault cases is more. The multi-resolution analysis (MRA) of wavelet transform is adopted for capturing the information about the nature of fault and location of fault. One end three-phase current of transmission line is measured and sampled. The error in the classification and location of the fault increased with overlapping of zones, which makes the proposed scheme very complex.

This paper is broadly classified into five parts: The first part gives the brief introduction and description of the related research work which has been already done. The second part deals with brief introduction of the projected algorithm. The second part also elaborates about the use of Clarke transform in detection of ground and Fourier transform and its application in calculation of phase shift angle. Third part deals with the generation of data set and development of fuzzy inference system (FIS) for segregation of faults on the basis of the ground. The GA-generalized neural network (GNN) is discussed in the fourth part. In the fifth part, model under consideration and its outcome are discussed, and the sixth part is conclusion. The results obtained by developed algorithm establish the authenticity of the proposed method. The flow of the algorithm is shown in Fig. 1.

Signal Processing and Information Gathering

The first step in the process of fault categorization is to acquire the appropriate signals, which gives the required information about the faults and is used in the process of fault detection and categorization. The unclassified information received from the analysis should be proper and precise enough for declaring exact nature of fault. Three-phase power transmission system has only two signals, which can be considered and analyzed. The first quantity is voltage, and the second quantity is current. In this paper, only the voltage signal of respective three phases is acquired at generating bus location and analyzed.

Application of Clarke Transform in Detection of Ground in Faults

The Clarke transformation (CT) is also known as $\alpha\beta\gamma$ transformation. This transform is generally used for analyzing three-phase quantities, which is similar to the symmetrical component analysis. The Clarke transformation of any three-phase quantity can be calculated as follows:

$$\begin{bmatrix} V_\alpha \\ V_\beta \\ V_\gamma \end{bmatrix} = \frac{2}{3} \begin{bmatrix} 1 & -\frac{1}{2} & -\frac{1}{2} \\ 0 & \frac{\sqrt{3}}{2} & -\frac{\sqrt{3}}{2} \\ \frac{1}{2} & \frac{1}{2} & \frac{1}{2} \end{bmatrix} \begin{bmatrix} V_a \\ V_b \\ V_c \end{bmatrix} \tag{1}$$

where V_a, V_b *and* V_c are any three-phase signal, and in the present case, they are voltages of three phases *a*, *b and c,* respectively. V_α, V_β *and* V_γ are three model components of Clarke transformation.

$$T = \frac{2}{3} \begin{bmatrix} 1 & -\frac{1}{2} & -\frac{1}{2} \\ 0 & \frac{\sqrt{3}}{2} & -\frac{\sqrt{3}}{2} \\ \frac{1}{2} & \frac{1}{2} & \frac{1}{2} \end{bmatrix} \tag{2}$$

where T is Clarke transformation matrix. The matrix T is unitary in nature, *i.e.,* its inverse is identical to its transpose.

The three model components of Clarke transformation provide the very useful information about the nature of fault. The first two components, *i.e.,* α-model component and β-model component, are related to the phase only and are known as real components. The last one, *i.e.,* γ-model component, is related to the ground only and hence known

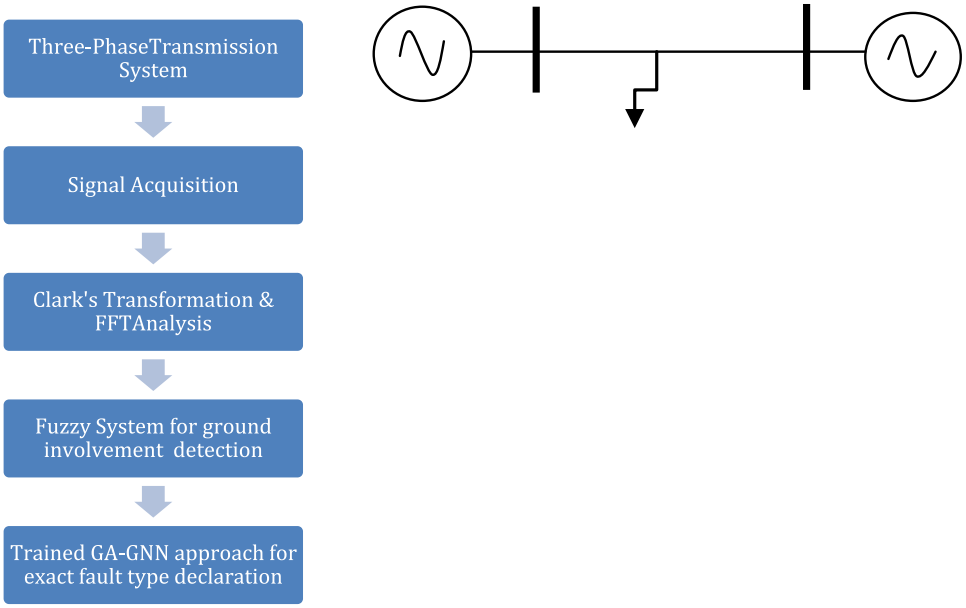

Fig. 1 Flow of fault classification system

as ground mode component. These components can be obtained easily with the help of Clarke transformation matrix as expressed in (1). The ground mode component of Clarke transformation is very identical to the symmetrical zero sequence component of three-phase voltages. This feature of Clarke transformation is effectively utilized in the detection of involvement of ground when any type of fault occurs.

In the present paper, the voltage signal of respective three phases is measured and first analyzed with the help of Clarke transformation. The three-phase measured voltage signals are then fed through the Clarke transformation block of MATLAB. Here, only the ground mode component V_γ is analyzed and used as an important input. The extensive study by simulating the model of transmission line shows that the magnitude of V_γ is very significant, whenever the ground is involved in any type of fault. The magnitude of V_γ is easily detectable and measurable, and this feature is adopted by the paper for segregation of ground-related faults from the phase-to-phase faults. The input matrix is formed by having the one dedicated row of the V_γ. The value of V_γ is obtained directly from the block available in the MATLAB. The mean of vector of V_γ generated in MATLAB is taken for each different value of transmission line parameters and different operating situations of power system. Hence, the phases-to-ground faults are easily distinguished by phase-to-phase faults.

Application of Fourier Transform in Calculating Phase Angle

The value of phase angle is an essential quantity associated with any of the electrical power system signal, whether voltage or current. Whenever any disturbance occurs in power system, phase angle also changes accordingly. The value of phase shift angle varies substantially from healthy power system to faulty power system. This holds true for all three phases of electrical power transmission system. The phase angle of voltage also changes with any fault or any disturbance on the transmission line. The change in phase angle of voltage or current of electrical power transmission system occurs because with any fault, the electrical topology of transmission network changes. This leads to an immediate change in X/R ratio of the transmission network, and hence, the phase angle changes accordingly.

The difference in the phase angle of voltage at different time intervals, *i.e.,* the pre-fault voltage and during-fault voltage, can be used for detection of fault. Hence, the changing pattern of phase angle alone can be used for the classification and detection of the faults. The value of phase angle may be negative or positive depending upon the time of sampling of the signal, which is three-phase voltage in the present case. The value of phase angle can be calculated in degrees, radians or in seconds, depending upon our convenience. This can be achieved simply by changing the settings of the MATLAB model of three-phase transmission line system. There are so many methods available for finding the phase angle, but the presented paper takes the help of fast Fourier transform (FFT) for calculating the phase angle. The FFT method of finding phase shift is very easy and suitable for sampled three-phase voltage signals.

The FFT of any signal y with n element is given by

$$Y_k = \sum_{j=0}^{n-1} w^{jk} y_j \tag{3}$$

where ω is a complex nth root of unity, *i.e.,*

$$w = \mathrm{e}^{-2\pi i/n} \tag{4}$$

The FFT can also be expressed with the help of matrix,

$$Y = Fy \tag{5}$$

The elements of F are given by the below equation:

$$f_{k,j} = \omega^{jk} \tag{6}$$

The nature of FFT matrix Y is complex for complex y.

Figure 2 shows the typical FFT windows (in red color) of phase voltage of phases A, B and C, respectively, for phase-to-ground fault, on phase A of the transmission line. Figure 3 shows the FFT analysis of all the waveforms, shown in Fig. 1 for all three-phase voltage signals. Table 1 shows the FFT parameters used for FFT analysis in the proposed research work. These waveforms are obtained by simulating the transmission line model developed in the MATLAB/Simulink environment for one combination of fault resistance and fault initiation angle. The FFT analysis of other voltages for different faults and different values of fault resistance and fault initiation angle is also carried out, but they are not shown here because of space constraint.

Fuzzy Decision System (FDS) for Segregation of the Ground Faults

The proposed research work has adopted the fuzzy logic for differentiating the faults which have ground involvement and which do not have involvement of the ground. The fuzziness in the data makes an effective implementation of the fuzzy logic in this method.

The fuzzy decision system mainly consists of the following components.

Fuzzification of the Analyzed Data

Fuzzification is a technique in which the input variables are mapped onto linguistic variables. These linguistic variables are then used by the fuzzy decision system (FDS) to make decisions of ground and non-ground fault classification. The output of Clark transformation (*i.e.,* ground mode component V_γ) is used as input to fuzzification block of FDS. The fuzzification process uses the membership functions to accomplish the task of fuzzification. Figure 4 shows the deployment of membership function for input variables.

Inference from the DATA

After fuzzification of the ground mode component, V_γ is mapped onto linguistic variables. The control decisions now can be made based on these linguistic variables in order to get the output in linguistic form. The input, *i.e.,* the ground mode component V_γ, is mapped in to three linguistic variables. The fuzzy input variable V_γ now consists of three linguistic variables, namely zero, positive and negative [i.e., zero (Z), positive (P) or negative (N)] depending upon the value of V_γ. Three simple fuzzy rules for fuzzy decision system formed are given as follows:

1. If V_γ is *Z,* then Fault *Non-Ground*
2. If V_γ is *P,* then Fault *Ground*
3. If V_γ is *N,* then Fault *Ground*

GA-Generalized Neural Network and Its Application in Fault Classification

The genetic algorithm-generalized neural network (GA-GNN) is a recent development in the field of intelligent tools, which is helpful in making meaningful decision from raw and unclassified data. Artificial neural network (ANN) was just one step earlier available for the same purpose. The ANN establishes a linear/nonlinear relationship in between input and output data or a universal function approximation to establish the relation in between input

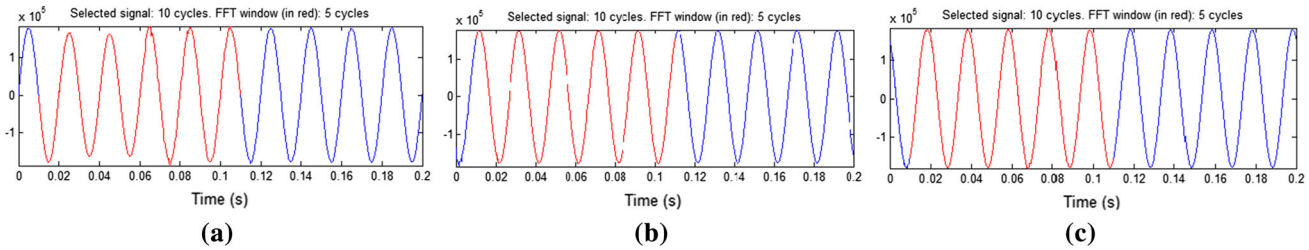

Fig. 2 FFT windows (in red color) for AG fault on three-phase transmission line. **a** Phase A voltage signal. **b** Phase B voltage signal. **c** Phase C voltage signal (color figure online)

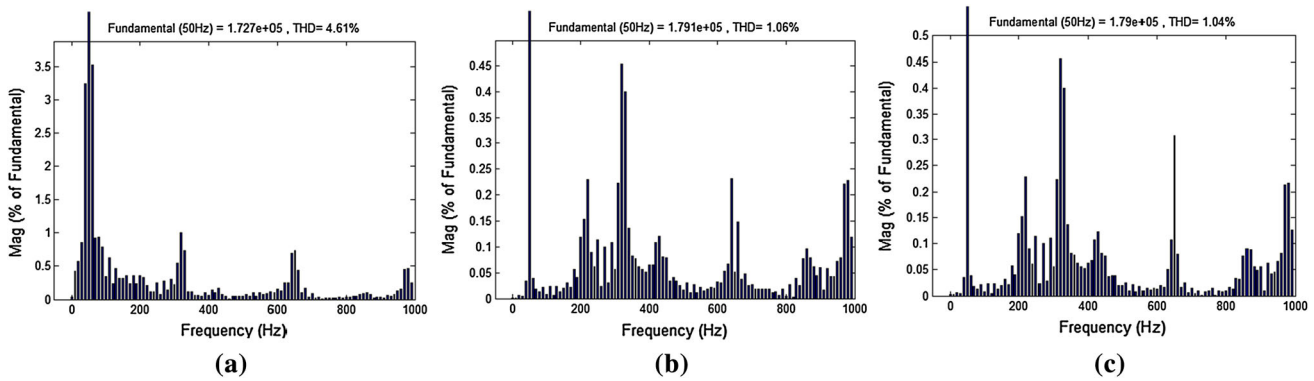

Fig. 3 FFT analysis of different phase voltages under AG fault on three-phase transmission line. **a** FFT of phase A voltage signal. **b** FFT of phase B voltage signal. **c** FFT of phase C voltage signal

Table 1 FFT parameters for FFT analysis

S. no.	Settings	Values
1	Start time	0.01 s
2	Number of cycles	5
3	Fundamental frequency	50 Hz
4	Maximum frequency	1000 Hz
	Maximum frequency for THD computation	Nyquist frequency

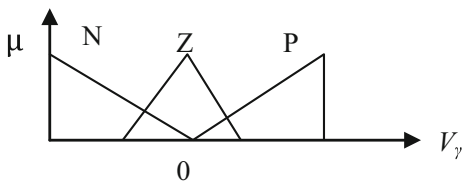

Fig. 4 Fuzzy membership functions for input variables

and output data. The aggregator functions used in developing ANN model is crisp in nature, which is not suitable for decision making, when we do not have input data in crisp form. Hence, the concept of GNN is developed which uses the compensatory operators which are fuzzy in nature and results are better as compared to ANN. Since the input data are fuzzy/vague in nature, the GNN uses the combination of sum and multiplication in order to deal with the vagueness of the input data.

Model of the GA-GNN

The presented paper has adopted two functions for developing the GA-GNN algorithm. The first is sigmoid function, and the second is Gaussian function. The combination of both provides the ability to deal with the nonlinearity involved in the problem. The typically developed GA-GNN model processes the output by summing up the output of sigmoid function and Gaussian function, and the proposed model is known as summation-type neural model.

The final output of the GA-GNN is a function of two outputs O_Σ and O_π, where Σ is summation function and π is aggregation function. The output of summation part is given by

$$O_\Sigma = \frac{1}{1 + e^{-\lambda_s * s\_net}} \tag{7}$$

where $s\_net = \Sigma W_i X_i + X_{o\Sigma}$ and λ_s = parameter of summation function.

The output of the product aggregation part can be represented as

$$O_\Pi = e^{-\lambda_p * p\_net^2} \tag{8}$$

where $p\_net = \Pi W_i X_i * X_{o\Pi}$ and λ_p = parameter of product function, and the final output of the GA-GNN is given by following equation:

$$\text{GA-GNNoutput} = O_\Sigma * W + O_\Pi * (1 - W) \tag{9}$$

This GA-GNN output is depending on weights factor (W). In this case, the weights are W and $(1 - W)$ for summation function and aggregation function, respectively.

Error Minimization Using GA

The output of the GA-GNN will contain error, and this error is calculated and minimized by comparing it with the desired output. The GA technique is adopted to minimize this error. Basically, the sum squared error for convergence of model is used. The sum squared error E_p is given by

$$E_p = \Sigma E_i^2 \tag{10}$$

where E_i is error, *i.e.*, $E_i^2 = (Y_i - O_i)$ between input Y_i and output O_i.

The change in weights (ΔW_Σ) with summation function and change in weights (ΔW_Π) with product function are find out using genetic algorithm.

The data matrix obtained by Clarke transforms and FFT is then used as input to the GA-GNN for various faults to

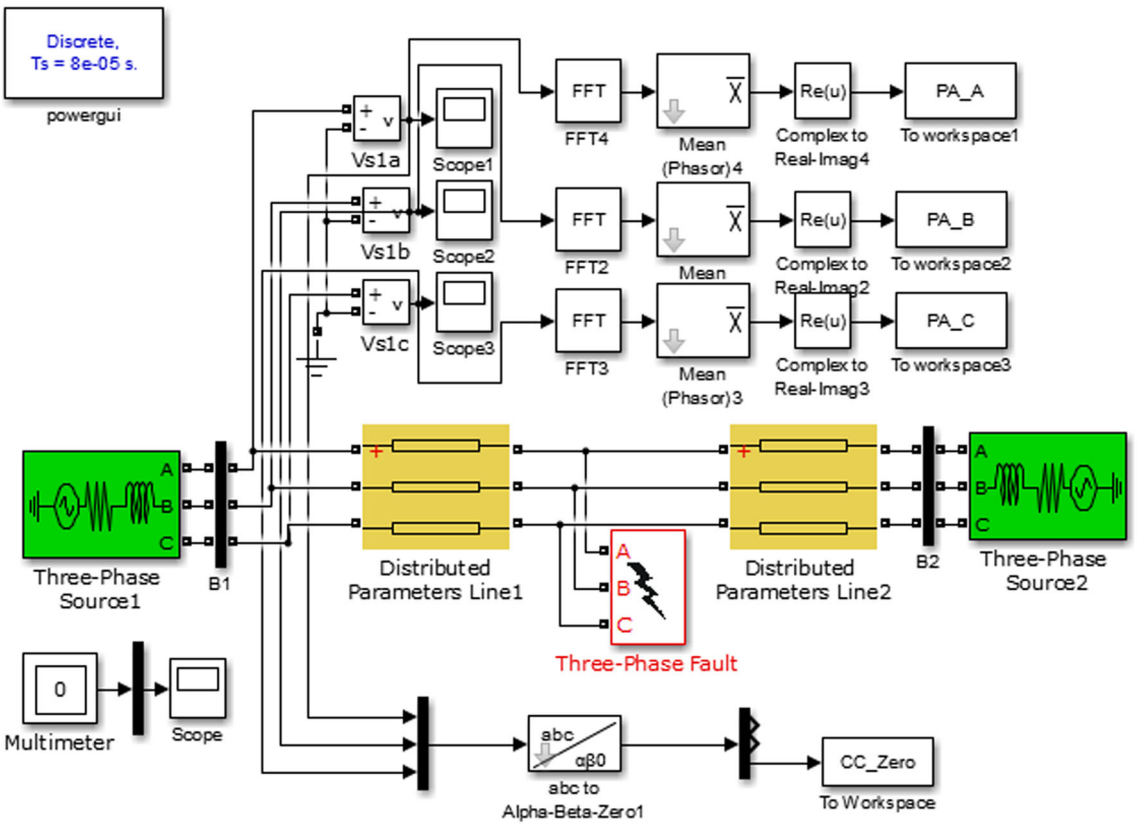

Fig. 5 Simulink model of the three-phase transmission line in MATLAB

train using GA. The GA-GNN model will then give the precise information about the kind of fault.

Modeling and Simulation of Three-Phase Transmission System

A three-phase transmission system model is created in the MATLAB for studying the diverse nature of the faults. The system under consideration has two generators connected at both the ends of the transmission line for energizing the line. The voltage of each phase is measured at the bus B1, as shown in Fig. 5. Clarke transformation is obtained with the help of Clarke transform block, instead of command line for detection of involvement of ground in the fault. Phase shift angle is also measured directly by using fast Fourier transform (FFT) block, which is readily available in the MATLAB. All of these blocks can be seen in Fig. 5. The value of ground fault resistance for all respective three phases is varied from 15 to 60 Ω, and for line faults, the fault resistance is varied from 0.10 to 0.75 Ω, respectively. These values provide a wide range of data over different operating conditions, and these data are utilized for generating the input matrix. The generated input matrix is then used for fuzzy logic and for training the GA-GNN model. The Fault commencement angle is very important factor as it plays a crucial role in deciding the magnitude of voltage at the time of fault, which also affects the during-fault voltage waveform. Hence, the value of fault commencement angle is varied from 0° to 90° so that all the possible situations can be taken into account. The sampling time taken is 80e−6 s, which covers all the signals of our interests.

The typical values of both the voltage sources are as follows:

Phase-to-phase RMS voltage: 220 kV
Number of phases: 3
Phase angle of phase at source A: 0°
Phase angle of phase at source A: 35°
Frequency: 50 Hz
Internal connection: Yg

The length of transmission line is 400 km, and distribution types of parameters are taken so that the needed accuracy can be obtained. Therefore, the given method can also be utilized for fault detection of long transmission line.

The fault resistances and fault inception angles are varied step by step. The model is simulated for each value of fault inception angle for extensive study of the phase voltage waveforms. Mean values of third component of

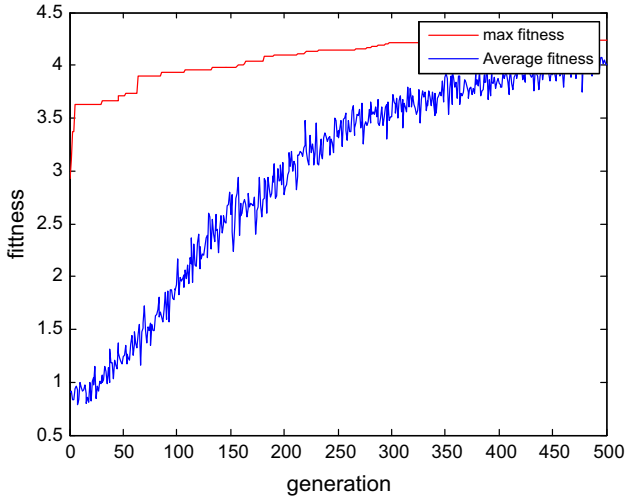

Fig. 6 Graph representing GA-GNN training

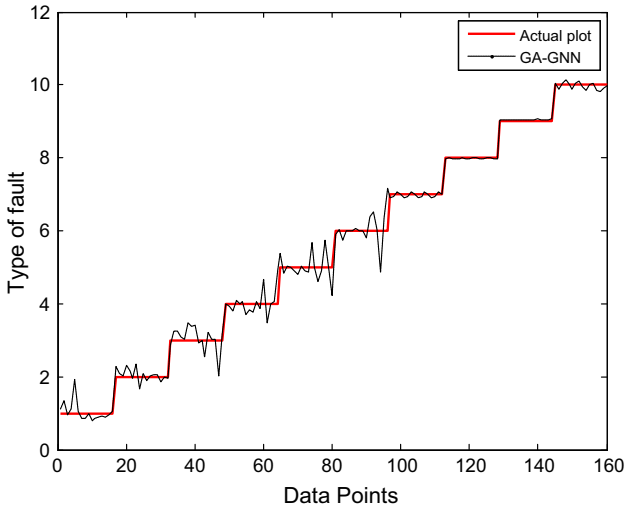

Fig. 7 Testing of GA-GNN for different types of faults

Clarke transform and phase shift angle are arranged in the matrix form. The matrix is normalized with respect to its own column so that the relative difference can be analyzed properly. The accuracy of the algorithm depends upon the training of the GA-GNN, which depends upon the size of the input data, *i.e.,* the more the size of input data, the better the accuracy of GA-GNN. The model is simulated for all possible ten types of fault for different parameters to generate the data set for training purpose of the GA-GNN. Figure 6 depicts the graph of GA-GNN training between generation and fitness of offspring. The graph represented in Fig. 7 shows the robustness of the proposed GA-GNN method for different types of faults. A GA-GNN and a typical ANN model structure are also compared here to show the simplicity of the proposed method shown in Table 2. The table shows the superiority of the proposed method.

Table 2 Comparison of network complexity involved in ANN and GA-GNN

S. no.	Components	ANN	GA-GNN
1	Structure of ANN/GN	(7–7–1)	(1)
2	Number of neurons used	08	01
3	Number of layers containing processing neurons	02	01
4	Number of interconnections	56	16

Results and Discussion

After training, the GA-GNN fault detector (FD) has been tested for different faulty conditions and different parameters. These conditions included different fault locations, different commencement angles from (*i.e.,* 0° to 90°) and different fault resistances (*i.e.,* 0 Ω to 60 Ω). Table 3 shows the variation in Clarke components and variation in phase angle for single-line-to-ground faults. It is clear that the value of V_γ for the ground-related fault is nonzero and is greater than values of V_γ for line-to-line faults. Table 4 shows the variation in Clarke components and variation in phase angle for double-line-to-ground faults, and Table 5 shows the variation in Clarke components and variation in phase angle for line-to-line faults. It is again clear that the value of V_γ for the faults, where the ground is not involved, is almost zero. The careful observation of the given tables can be concluded in the form that for each type of fault a unique pattern of data is generated. These unique patterns can be used for classification of faults. Based upon these data, an artificial intelligent network is developed.

Conclusion

This paper proposed a GA-GNN method for fault categorization of a three-phase transmission system. The paper has adopted the Clarke transform, phase shift angle, fuzzy logic and GA-GNN efficiently for categorization of faults of a three-phase transmission system. The voltage signals at one bus of the transmission system are used for fault categorization, and this makes the adaption and realistic implementation of the algorithm effortless. The effectiveness and preciseness of the presented method have been increased by synergizing the qualities of both fuzzy logic and GA-GNN. The training data set of GA-GNN for diverse realistic conditions, *e.g.,* fault commencement angle, fault resistance and ten different types of faults GA-

Table 3 Changing patterns of Clarke component and phase angle variation for different values of fault resistances and fault commencement angle for single-phase-to-ground faults

Type of fault	Fault resistance	Fault inception angle	Clarke component (V_γ)	Phase angle of phase A	Phase angle of phase B	Phase angle of phase C
1. AG	R_f = 15 Ω	0°	− 7.43632	− 21.487	− 0.82552	0.000813
		30°	− 4.29981	− 12.3686	− 0.68003	0.146296
		60°	− 17.4981	− 50.8091	− 1.2704	− 0.44407
		90°	− 8.38389	− 24.2917	− 0.85704	− 0.03071
	R_f = 30 Ω	0°	− 2.48496	− 7.13907	− 0.57713	0.2492
		30°	− 0.60912	− 1.68517	− 0.49044	0.335892
		60°	− 12.4564	− 35.9488	− 1.11839	− 0.29206
		90°	− 6.98213	− 20.017	− 0.87334	− 0.04701
	R_f = 45 Ω	0°	− 1.06843	− 2.94876	− 0.54569	0.280642
		30°	− 12.6321	− 36.4011	− 1.15234	− 0.32601
		60°	− 9.59663	− 27.6263	− 0.98594	− 0.15961
		90°	− 5.69345	− 16.2707	− 0.80958	0.016744
	R_f = 60 Ω	0°	− 0.5372	− 1.37369	− 0.53656	0.289773
		30°	− 10.1129	− 29.1429	− 1.00549	− 0.17916
		60°	− 7.7507	− 22.3115	− 0.87751	− 0.05118
		90°	− 4.72153	− 13.5038	− 0.73814	0.088193
BG	R_f = 15 Ω	0°	17.21781	0.949106	49.57504	1.150883
		30°	8.525463	0.55404	24.29017	0.755817
		60°	− 0.13238	0.090703	− 0.76025	0.29248
		90°	− 5.99181	− 0.17765	− 17.7998	0.024123
	R_f = 30 Ω	0°	12.27834	0.780278	35.08592	0.982055
		30°	7.056711	0.548366	19.88727	0.750143
		60°	1.892149	0.265995	4.954851	0.467772
		90°	− 1.63015	0.108262	− 5.29431	0.310039
	R_f = 45 Ω	0°	9.462818	0.625329	26.95037	0.827106
		30°	5.740247	0.459532	16.11569	0.661309
		60°	2.050611	0.258375	5.446916	0.460152
		90°	− 0.46084	0.145314	− 1.85983	0.347091
	R_f = 60 Ω	0°	7.647462	0.514558	21.7208	0.716335
		30°	4.759428	0.384699	13.31674	0.586476
		60°	1.884322	0.229524	5.000935	0.431301
		90°	− 0.06372	0.140508	− 0.66451	0.342285
CG	R_f = 15 Ω	0°	0.363857	0.17208	− 0.45247	1.390531
		30°	5.921776	0.42419	− 0.20036	17.55754
		60°	7.467999	0.511377	− 0.11317	22.02287
		90°	4.212039	0.351194	− 0.27336	12.57622
	R_f = 30 Ω	0°	− 1.75265	0.023502	− 0.60105	− 4.67279
		30°	1.587774	0.16991	− 0.45464	5.054913
		60°	2.508955	0.22424	− 0.40031	7.710155
		90°	0.561267	0.12745	− 0.4971	2.061494
	R_f = 45 Ω	0°	− 1.94706	0.044837	− 0.57972	− 5.317
		30°	0.434242	0.149149	− 0.4754	1.618092
		60°	1.091619	0.188264	− 0.43629	3.512177
		90°	12.59865	0.809316	0.184764	36.78387
	R_f = 60 Ω	0°	− 1.80237	0.071241	− 0.55331	− 4.93525
		30°	0.04483	0.152911	− 0.47164	0.443367
		60°	0.55686	0.183216	− 0.44134	1.918858
		90°	10.08241	0.672766	0.048214	29.52576

Table 4 Changing patterns of Clarke component and phase angle variation for different values of fault resistances and fault commencement angle for double-phase-to-ground faults

Type of fault	Fault resistance	Fault commencement angle	Clarke component (V_γ)	Phase angle of phase A	Phase angle of phase B	Phase angle of phase C
ABG	R_f = 15 Ω	0°	12.01572	− 18.7832	53.88802	0.960756
		30°	− 12.2634	− 89.0291	52.53426	− 0.32565
		60°	− 13.462	− 59.2376	19.19126	− 0.36802
		90°	− 10.9397	− 25.505	− 7.09985	− 0.24278
	R_f = 30 Ω	0°	10.26322	− 5.87821	35.84682	0.838179
		30°	− 7.47502	− 54.5167	32.15973	− 0.04445
		60°	− 8.26454	− 39.4121	14.71542	− 0.07268
		90°	− 6.60516	− 21.5274	1.720555	0.015611
	R_f = 45 Ω	0°	8.274744	− 3.17339	27.27879	0.739038
		30°	− 5.48493	− 39.2582	22.77167	0.058726
		60°	− 6.07357	− 29.1713	10.9391	0.038699
		90°	− 4.83611	− 16.9466	2.360436	0.105588
	R_f = 60 Ω	0°	6.845024	− 2.01123	21.90129	0.658821
		30°	− 4.38911	− 30.7045	17.45008	0.107773
		60°	− 4.85795	− 23.1411	8.495162	0.092786
		90°	− 3.87047	− 13.8449	2.108089	0.146506
BCG	R_f = 15 Ω	0°	13.43092	0.866106	57.688	− 18.2253
		30°	11.00158	0.739274	25.53177	6.771412
		60°	5.471301	0.487618	− 3.08085	19.04646
		90°	− 1.59474	0.111219	− 18.6903	13.83134
	R_f = 30 Ω	0°	8.227535	0.548825	38.46962	− 14.3104
		30°	6.628956	0.457437	21.42561	− 1.97089
		60°	2.988338	0.30225	5.506595	3.182848
		90°	− 1.6557	0.04494	− 4.00691	− 0.98063
	R_f = 45 Ω	0°	6.047365	0.445852	28.49002	− 10.791
		30°	4.855566	0.375069	16.83942	− 2.64515
		60°	2.145016	0.263984	5.742179	0.432383
		90°	11.62611	0.695175	− 2.89268	37.04688
	R_f = 60 Ω	0°	4.838344	0.3901	22.55435	− 8.42934
		30°	3.886786	0.332307	13.69357	− 2.36532
		60°	1.731305	0.246578	5.160442	− 0.21286
		90°	9.509379	0.583351	− 1.71136	29.64832
CAG	R_f = 15 Ω	0°	− 5.27678	− 18.7743	− 0.82418	3.803945
		30°	1.462544	− 13.689	− 0.45016	18.56223
		60°	− 12.1937	− 55.2496	− 1.12094	19.73739
		90°	12.33687	− 52.4125	0.161457	89.21551
	R_f = 30 Ω	0°	− 2.85018	− 2.67589	− 0.63838	− 5.24785
		30°	1.579358	1.348168	− 0.37923	3.757228
		60°	− 10.3962	− 36.6978	− 0.9889	6.504368
		90°	7.505168	− 32.3033	− 0.08812	54.88591
	R_f = 45 Ω	0°	− 2.03438	0.133353	− 0.6048	− 5.6458
		30°	− 11.6725	− 36.6839	− 1.02087	2.702924
		60°	− 8.38057	− 27.9349	− 0.89097	3.699613
		90°	5.496696	− 22.9022	− 0.20353	39.59814
	R_f = 60 Ω	0°	− 1.64031	0.763033	− 0.58883	− 5.11149
		30°	− 9.55129	− 29.2822	− 0.90885	1.546112
		60°	− 6.92787	− 22.4742	− 0.80877	2.508395
		90°	4.397494	− 17.6008	− 0.25032	31.04853

Table 5 Patterns of Clarke component and phase angle variation for different values of fault resistances and fault commencement angle for line-to-line fault

Type of fault	Fault resistance	Fault commencement angle	Clarke component (V_γ)	Phase angle of phase A	Phase angle of phase B	Phase angle of phase C
AB	R_f = 0.10 Ω	0°	6.63E−05	− 386.323	385.9802	0.342539
		30°	1.29E−05	− 185.129	184.7863	0.342663
		60°	− 0.00039	− 24.4835	24.13855	0.343813
		90°	− 0.00035	258.5644	− 258.909	0.343678
	R_f = 0.25 Ω	0°	6.81E−05	− 363.51	363.1675	0.342533
		30°	1.39E−05	− 171.935	171.592	0.342658
		60°	− 0.00039	− 24.7038	24.35876	0.343813
		90°	− 0.00035	242.76	− 243.105	0.343683
	R_f = 0.50 Ω	0°	6.98E−05	− 328.986	328.644	0.342528
		30°	1.39E−05	− 152.097	151.754	0.342658
		60°	− 0.00039	− 25.3256	24.98066	0.343813
		90°	− 0.00035	218.7616	− 219.106	0.343693
	R_f = 0.75 Ω	0°	7.27E−05	− 298.381	298.0384	0.342517
		30°	1.39E−05	− 134.68	134.337	0.342658
		60°	− 0.00039	− 26.1686	25.82359	0.343813
		90°	− 0.00035	197.4177	− 197.762	0.343697
BC	R_f = 0.10 Ω	0°	3.93E−04	0.139817	13.86568	− 14.0043
		30°	3.49E−04	0.139943	− 255.501	255.3623
		60°	0.000259	0.140216	− 442.489	442.3496
		90°	0.000153	0.140507	− 489.051	488.9114
	R_f = 0.25 Ω	0°	3.92E−04	0.139819	14.6574	− 14.796
		30°	3.50E−04	0.139937	− 239.903	239.7644
		60°	0.000264	0.1402	− 417.115	416.9759
		90°	0.000157	0.140491	− 461.39	461.2505
	R_f = 0.50 Ω	0°	3.92E−04	0.139819	16.1346	− 16.2732
		30°	3.52E−04	0.139932	− 216.214	216.0747
		60°	0.000267	0.140185	− 378.594	378.4547
		90°	0.000164	0.140467	− 419.367	419.2271
	R_f = 0.75 Ω	0°	3.92E−04	0.139819	17.72424	− 17.8629
		30°	3.53E−04	0.139927	− 195.133	194.9945
		60°	0.00027	0.140172	− 344.345	344.2056
		90°	0.000165	0.14046	− 381.971	381.831
CA	R_f = 0.10 Ω	0°	− 2.56E−04	− 445.432	− 0.48294	445.9145
		30°	− 1.54E−04	− 488.698	− 0.4832	489.1812
		60°	− 6.81E−05	− 392.044	− 0.48346	392.5274
		90°	− 1.28E−05	− 181.335	− 0.48359	181.8188
	R_f = 0.25 Ω	0°	− 2.60E−04	− 419.904	− 0.48292	420.3857
		30°	− 1.59E−04	− 461.039	− 0.48319	461.5214
		60°	− 6.99E−05	− 368.95	− 0.48345	369.4335
		90°	− 1.28E−05	− 168.293	− 0.48359	168.7761
	R_f = 0.50 Ω	0°	− 2.64E−04	− 381.161	− 0.48291	381.6435
		30°	− 1.65E−04	− 419.031	− 0.48316	419.5135
		60°	− 7.32E−05	− 333.981	− 0.48344	334.4645
		90°	− 1.38E−05	− 148.714	− 0.48358	149.1977
	R_f = 0.75 Ω	0°	− 2.67E−04	− 346.711	− 0.4829	347.1929
		30°	− 1.69E−04	− 381.666	− 0.48315	382.1488
		60°	− 7.46E−05	− 302.969	− 0.48343	303.452
		90°	− 1.38E−05	− 131.525	− 0.48358	132.0082

GNN, made the method more robust. The training time taken for the GA-GNN is comparatively less. The results obtained show that the presented scheme is very effective and robust in classification of the different types of fault. All efforts have been made in the modeling of the three-phase transmission system to match with the real-life transmission system.

References

1. M.S. Abdel Aziz, M.A. Moustafa Hassan, E.A. Zahab, High-impedance faults analysis in distribution networks using an adaptive neuro fuzzy inference system. Electr. Power Compon. Syst. **40**, 1300–1318 (2012)
2. S.R. Samantaray, A systematic fuzzy rule based approach for fault classification in transmission lines. Appl. Soft Comput. **13**, 928–938 (2013)
3. A. Dasgupta, S. Nath, A. Das, Transmission line fault classification and location using wavelet entropy and neural network. Electr. Power Compon. Syst. **40**(15), 1676–1689 (2012)
4. M. Jamila, A. Kalam, A.Q. Ansaria, M. Rizwan, Generalized neural network and wavelet transform based approach for fault location estimation of a transmission line. Appl. Soft Comput. **19**, 322–332 (2014)
5. A.K. Pradhan, A. Routrsy, S. Pati, D.K. Pradhan, Wavelet fuzzy combined approach for fault classification of a series compensated transmission line. IEEE Trans. Power Deliv. **19**(4), 1612–1618 (2004)
6. C.K. Jung, K.H. Kim, J.B. Lee, B. Klöckl, Wavelet and neuro-fuzzy based fault location for combined transmission systems. Int. J. Electr. Power Energy Syst. **29**, 445–454 (2007)
7. D.K. Chaturvedi, *Soft computing techniques and its applications in electrical engineering* (Springer, Berlin, 2008)
8. D.K. Chaturvedi, P.S. Satsangi, P.K. Kalra, Neuro fuzzy approach for development of new neuron model. Soft Comput. **8**, 19–27 (2003)
9. J. Sadeh, H. Afradi, A new and accurate fault location algorithm for combined transmission lines using adaptive network-based fuzzy inference system. Electr. Power Syst. Res. **79**, 538–1545 (2009)
10. Z. Moravej, A.A. Abdoos, M. Sanaye-Pasand, A new approach based on s-transform for discrimination and classification of inrush current from internal fault currents using probabilistic neural network. Electr. Power Compon. Syst. **38**, 1194–1210 (2010)
11. M.J. Reddy, D.K. Mohanta, A wavelet-neuro-fuzzy combined approach for digital relaying of transmission line faults. Electr. Power Compon. Syst. **35**, 1385–1407 (2007)
12. M. Rizwan, M.A. Kalam, M. Jamil, A.Q. Ansari, Wavelet-FFNN based fault location estimation of a transmission line. Electr. Eng. Res. (EER) Int. Refereed J. USA **1**(3): 77–82, 2013. ISSN: 2327-7254 (print), 2327-7564
13. E.A. Alanzi, M.A. Younis, A.M. Ariffin, Detection of faulted phase type in distribution systems based on one end voltage measurement. Electr. Power Energy Syst. **54**, 288–292 (2014)